Vegetable Research

ARTICLE

Open Access

https://doi.org/10.48130/VR-2023-0010
*Vegetable Research* **2023**, 3:10

# Aquaporin genes in garden pea and their regulation by the nano-antioxidant fullerol in imbibing embryos under osmotic stress

Arun Kumar Pandey[1#], Ting Sun[1,2#], Xinyang Wu[1], Zhuoyi Wang[1], Rujia Jiang[1], Peipei Zhang[1,2], Pingping Fang[1,2] and Pei Xu[1,2*]

[1] *College of Life Sciences, China Jiliang University, Hangzhou 310018, China*
[2] *Key Laboratory of Specialty Agri-Product Quality and Hazard Controlling Technology of Zhejiang Province, Hangzhou 310018, China*
[#] These authors contributed equally: Arun Kumar Pandey, Ting Sun
[*] Corresponding author, E-mail: peixu@cjlu.edu.cn

## Abstract

Aquaporins (AQPs) are known as small membrane intrinsic proteins that help to transport water and certain solutes through biological membranes. AQPs gene families have been extensively studied in major crops, but less investigated in pea (*Pisum sativum* L.), which is an economically significant legume crop with a huge complex genome. Here, we present a genome-wide identification, structural characterization, subcellular localization, and expression profiling of the AQPs in pea with a particular interest in their involvement in nano fullerol-conferred osmotic stress alleviation. We identified 39 full-length aquaporin genes from the pea genome, which were classified into five subfamilies. The protein structure of aquaporins appears to have substrate-specific residues which are conserved in plants, allowing for inference of substrate specificity. In particular, PsNIP2-2-2 was identified with a Gly-Ser-Gly-Arg (GSGR) selective filter that indicates the ability to uptake silicon. Analysis of tissue transcriptomes revealed preferred expressions of certain *PsAQPs* in the underground, aerial and reproductive organs, respectively. Development-regulated expression of two *PsTIPs* and two *PsPIPs* in seeds were noticed. RNA-Seq of the imbibing embryos treated with mannitol (M) or mannitol plus 100 mg/L fullerol (MF) revealed two *PsTIPs* being similarly regulated by M or MF, three *PsNIPs* being up-regulated only by M without F, and four other genes that were only regulated under MF condition. To our knowledge, this is the first report on transcriptional regulation of AQPs by fullerols, which adds to our knowledge on the plant-carbon nano-substances interactions.

**Citation:** Pandey AK, Sun T, Wu X, Wang Z, Jiang R, et al. 2023. Aquaporin genes in garden pea and their regulation by the nano-antioxidant fullerol in imbibing embryos under osmotic stress. *Vegetable Research* 3:10 https://doi.org/10.48130/VR-2023-0010

## INTRODUCTION

Aquaporin's (AQPs) are small (21–34 kD) channel-forming, water-transporting trans-membrane proteins which are known as membrane intrinsic proteins (MIPs) conspicuously present across all kingdoms of life. In addition to transporting water, plant AQPs act to transport other small molecules including ammonia, carbon dioxide, glycerol, formamide, hydrogen peroxide, nitric acid, and some metalloids such as boron and silicon from the soil to different parts of the plant[1]. AQPs are typically composed of six or fewer transmembrane helices (TMHs) coupled by five loops (A to E) and cytosolic N- and C-termini, which are highly conserved across taxa[2]. Asparagine-Proline-Alanine (NPA) boxes and makeup helices found in loops B (cytosolic) and E (non-cytosolic) fold back into the protein's core to form one of the pore's two primary constrictions, the NPA region[1]. A second filter zone exists at the pore's non-cytosolic end, where it is called the aromatic/arginine (ar/R) constriction. The substrate selectivity of AQPs is controlled by the amino acid residues of the NPA and ar/R filters as well as other elements of the channel[1].

To date, the AQP gene families have been extensively explored in the model as well as crop plants[3–9]. In seed plants, AQP distributed into five subfamilies based on subcellular localization and sequence similarities: the plasma membrane intrinsic proteins (PIPs; subgroups PIP1 and PIP2), the tonoplast intrinsic proteins (TIPs; TIP1-TIP5), the nodulin26-like intrinsic proteins (NIPs; NIP1-NIP5), the small basic intrinsic proteins (SIPs; SIP1-SIP2) and the uncategorized intrinsic proteins (XIPs; XIP1-XIP3)[2,10]. Among them, TIPs and PIPs are the most abundant and play a central role in facilitating water transport. SIPs are mostly found in the endoplasmic reticulum (ER)[11], whereas NIPs homologous to GmNod26 are localized in the peribacteroid membrane[12].

Several studies reported that the activity of AQPs is regulated by various developmental and environmental factors, through which water fluxes are controlled[13]. AQPs are found in all organs such as leaves, roots, stems, flowers, fruits, and seeds[14,15]. According to earlier studies, increased AQP expression in transgenic plants can improve the plants' tolerance to stresses[16,17]. Increased root water flow caused by upregulation of root aquaporin expression may prevent transpiration[18,19]. Overexpression of *Tamarix hispida ThPIP2:5* improved osmotic stress tolerance in *Arabidopsis* and *Tamarix* plants[20]. Transgenic tomatoes having apple *MdPIP1;3* ectopically expressed produced larger fruit and improved drought tolerance[21]. Plants over-expressing heterologous AQPs, on the other hand, showed negative effects on stress tolerance in many cases. Overexpression of *GsTIP2;1* from *G. soja* in *Arabidopsis* plants exhibited lower resistance against salt and drought stress[22].

A few recent studies have started to establish a link between AQPs and nanobiology, a research field that has been

accelerating in the past decade due to the recognition that many nano-substances including carbon-based materials are valuable in a wide range of agricultural, industrial, and biomedical activities[23]. Carbon nanotubes (CNTs) were found to improve water absorption and retention and thus enhance seed germination in tomatoes[24,25]. Ali et al.[26] reported that Carbon nanoparticles (CTNs) and osmotic stress utilize separate processes for AQP gating. Despite lacking solid evidence, it is assumed that CNTs regulate the aquaporin (AQPs) in the seed coats[26]. Another highly noticed carbon-nano-molecule, the fullerenes, is a group of allotropic forms of carbon consisting of pure carbon atoms[27]. Fullerenes and their derivatives, in particular the water-soluble fullerols [$C_{60}(OH)_{20}$], are known to be powerful antioxidants, whose biological activity has been reduced to the accumulation of superoxide and hydroxyl[28,29]. Fullerene/fullerols at low concentrations were reported to enhance seed germination, photosynthesis, root growth, fruit yield, and salt tolerance in various plants such as bitter melon and barley[30–32]. In contrast, some studies also reported the phytotoxic effect of fullerene/fullerols[33,34]. It remains unknown if exogenous fullerene/fullerol has any impact on the expression or activity of AQPs in the cell.

Garden pea (*P. sativum*) is a cool-season crop grown worldwide; depending on the location, planting may occur from winter until early summer. Drought stress in garden pea mainly affects the flowering and pod filling which harm their yield. In the current study, we performed a genome-wide identification and characterization of the AQP genes in garden pea (*P. sativum*), the fourth largest legume crop worldwide with a large complex genome (~4.5 Gb) that was recently decoded[35]. In particular, we disclose, for the first time to our best knowledge, that the transcriptional regulations of AQPs by osmotic stress in imbibing pea seeds were altered by fullerol supplement, which provides novel insight into the interaction between plant AQPs, osmotic stress, and the carbon nano-substances.

## MATERIALS AND METHODS

### Identification of AQP genes through Genome-wide

The whole-genome sequence of garden pea ('Caméor') was retrieved from the URGI Database (https://urgi.versailles.inra.fr/Species/Pisum). Protein sequences of AQPs from two model crops (Rice and Arabidopsis) and five other legumes (Soybean, Chickpea, Common bean, Medicago, and Peanut) were used to identify homologous AQPs from the garden pea genome (Supplemental Table S1). These protein sequences, built as a local database, were then BLASTp searched against the pea genome with an *E*-value cutoff of $10^{-5}$ and hit a score cutoff of 100 to identify AQP orthologs. The putative AQP sequences of pea were additionally validated to confirm the nature of MIP (Supplemental Table S2) and transmembrane helical domains through TMHMM (www.cbs.dtu.dk/services/TMHMM/).

### Phylogenetic analysis and classification of AQP genes

Further phylogenetic analysis was performed to categorize the AQPs into subfamilies. The pea AQP amino acid sequences, along with those from Medicago, a cool-season model legume phylogenetically close to pea, were aligned through ClustalW2 software (www.ebi.ac.uk/Tools/msa/clustalw2) to assign protein names. The unaligned AQP sequences to Medicago counterparts were once again aligned with the AQP sequences of Arabidopsis, rice, and soybean. Based on the LG model, unrooted phylogenetic trees were generated *via* MEGA7 and the neighbor-joining method[36], and the specific name of each AQP gene was assigned based on its position in the phylogenetic tree.

### Analysis of the NPA motif and transmembrane domains

By using the conserved domain database (CDD, www.ncbi.nlm.nih.gov/Structure/cdd/cdd.shtml), the NPA motifs were identified from the pea AQP protein sequences[37]. The software TMHMM (www.cbs. dtu.dk/services/TMHMM/)[38] was used to identify the protein transmembrane domains. To determine whether there were any alterations or total deletion, the transmembrane domains were carefully examined.

### Characterization of AQP genes and protein properties

Basic molecular properties including amino acid composition, relative molecular weight (MW), and instability index were investigated through the online tool ProtParam (https://web.expasy.org/protparam/). The isoelectric points (pI) were estimated by sequence Manipulation Suite version 2 (www.bioinformatics.org/sms2)[39]. The subcellular localization of AQP proteins was predicted using Plant-mPLoc[40] and WoLF PSORT (www.genscript.com/wolf-psort.html)[41] algorithms.

The gene structure (intron-exon organization) of *AQPs* was examined through GSDS ver 2.0[42]. The chromosomal distribution of the *AQP* genes was illustrated by the software MapInspect (http://mapinspect.software.informer.com) in the form of a physical map.

### *In silico* tissue expression profiling of AQPs genes

To explore the tissue expression patterns of pea AQP genes, existing NGS data from 18 different libraries covering a wide range of tissue, developmental stage, and growth condition of the variety 'Caméor' were downloaded from GenBank (www.ncbi.nlm.nih.gov/bioproject/267198). The expression levels of the AQP genes in each tissue and growth stage/condition were represented by the FPKM (Fragments Per Kilobase of transcript per Million fragments mapped) values. Heatmaps of AQPs gene were generated through Morpheus software (https://software.broadinstitute.org/morpheus/#).

### Plant material and seed treatment with different substances

Different solutions, which were water (W), 0.3 M mannitol (M), and fullerol of different concentrations dissolved in 0.3 M mannitol (MF), were used in this study. MF solutions with the fullerol concentration of 10, 50, 100, and 500 mg/L were denoted as MF1, MF2, MF3, and MF4, respectively. Seeds of 'SQ-1', a Chinese landrace accession of a pea, were germinated in two layers of filter paper with 30 mL of each solution in Petri dishes (12 cm in diameter) each solution, and the visual phenotype and radicle lengths of 150 seeds for each treatment were analyzed 72 h after soaking. The radicle lengths were measured using a ruler. Multiple comparisons for each treatment were performed using the SSR-Test method with the software SPSS 20.0 (IBM SPSS Statistics, Armonk, NY, USA).

### RNA-Seq of imbibing embryos and data analysis

Total RNA was extracted from imbibing embryos after 12 h of seed soaking in the W, M, and MF3 solution, respectively, by using Trizol reagent (Invitrogen, Carlsbad, CA, USA). The quality

and quantity of the total RNA were measured through electrophoresis on 1% agarose gel and an Agilent 2100 Bioanalyzer respectively (Agilent Technologies, Santa Rosa, USA). The TruSeq RNA Sample Preparation Kit was utilized to construct an RNA-Seq library from 5 μg of total RNA from each sample according to the manufacturer's instruction (Illumina, San Diego, CA, USA). Next-generation sequencing of nine libraries were performed through Novaseq 6000 platform (Illumina, San Diego, CA, USA).

First of all, by using SeqPrep (https://github.com/jstjohn/SeqPrep) and Sickle (https://github.com/najoshi/sickle) the raw RNA-Seq reads were filtered and trimmed with default parameters. After filtering, high-quality reads were mapped onto the pea reference genome (https://urgi.versailles.inra.fr/Species/Pisum) by using TopHat (V2.1.0)[43]. Using Cufflinks, the number of mapped reads from each sample was determined and normalised to FPKM for each predicted transcript (v2.2.1). Pairwise comparisons were made between W *vs* M and W *vs* M+F treatments. The DEGs with a fold change ≥ 1.5 and false discovery rate (FDR) adjusted *p*-values ≤ 0.05 were identified by using Cuffdiff[44].

### Quantitative real-time PCR (qRT-PCR )

qPCR was performed by using TOROGGreen® qPCR Master Mix (Toroivd, Shanghai, China) on a qTOWER®3 Real-Time PCR detection system (Analytik Jena, Germany). The reactions were performed at 95 °C for 60 s, followed by 42 cycles of 95 °C for 10 s and 60 °C for 30 s. Quantification of relative expression level was achieved by normalization against the transcripts of the housekeeping genes $\beta$-tubulin according to Kreplak et al.[35]. The primer sequences for reference and target genes used are listed in Supplemental Table S3.

## RESULTS

### Identification and classification of the AQP genes in garden pea

The homology-based analysis identifies 41 putative AQPs in the garden pea genome. Among them, all but two genes (*Psat0s3550g0040.1*, *Psat0s2987g0040.1*) encode full-length aquaporin-like sequences (Table 1). The conserved protein domain analysis later validated all of the expected AQPs (Supplemental Table S2). To systematically classify these genes and elucidate their relationship with the AQPs from other plants' a phylogenetic tree was created. It clearly showed that the AQPs from pea and its close relative M. *truncatula* formed four distinct clusters, which represented the different subfamilies of AQPs *i.e.* TIPs, PIPs, NIPs, and SIPs (Fig. 1a). However, out of the 41 identified pea AQPs, 4 AQPs couldn't be tightly aligned with the Medicago AQPs and thus were put to a new phylogenetic tree constructed with AQPs from rice, Arabidopsis, and soybean. This additional analysis assigned one of the 4 AQPs to the XIP subfamily and the rest three to the TIP or NIP subfamilies (Fig. 1b). Therefore, it is concluded that the 41 PsAQPs comprise 11 PsTIPs, 15 PsNIPs, 9 PsPIPs, 5 PsSIPs, and 1 PsXIP (Table 2). The PsPIPs formed two major subgroups namely PIP1s and PIP2s, which comprise three and six members, respectively (Table 1). The PsTIPs formed two major subgroups TIPs 1 (PsTIP1-1, PsTIP1-3, PsTIP1-4, PsTIP1-7) and TIPs 2 (PsTIP2-1, PsTIP2-2, PsTIP2-3, PsTIP2-6) each having four members (Table 2). Detailed information such as gene/protein names, accession numbers, the length of deduced polypeptides, and protein structural features are presented in Tables 1 & 2

### Genome distribution and gene structure analysis of pea AQPs

To understand the genome distribution of the 41 *PsAQPs*, we mapped these genes onto the seven chromosomes of a pea to retrieve their physical locations (Fig. 2). The greatest number (10) of *AQPs* were found on chromosome 7, whereas the least (2) on chromosome 4 (Fig. 2 and Table 1). Chromosomes 1 and 6 each contain six aquaporin genes, whereas chromosomes 2, 3, and 5 carry four, seven, and four aquaporin genes, respectively (Fig. 2). The trend of clustered distribution of AQPs was seen on specific chromosomes, particularly near the end of chromosome 7.

The 39 full-length PsAQP proteins have a length of amino acid ranging from 115 to 503 (Table 1) and Isoelectric point (pI) values ranging from 4.72 to 10.35 (Table 2). As a structural signature, transmembrane domains were predicted to exist in all PsAQPs, with the number in individual AQPs varying from 2 to 6. By subfamilies, TIPs harbor the greatest number of TM domains in total, followed by PIPs, NIPs, SIPs, and XIP (Table 2). Exon-intron structure analysis showed that most *PsAQPs* (16/39) having two introns, while ten members had three, seven members had four, and five members had only one intron (Fig. 3). Overall, *PsAQPs* exhibited a complex structure with varying intron numbers, positions, and lengths.

### Characterization of the NPA motifs

As aforementioned, generally highly conserved two NPA motifs generate an electrostatic repulsion of protons in AQPs to form the water channel, which is essential for the transport of substrate molecules[15]. In order to comprehend the potential physiological function and substrate specificity of pea aquaporins, NPA motifs (LB, LE) and residues at the ar/R selectivity filter (H2, H5, LE1, and LE2) were examined. (Table 2). We found that all PsTIPs and most PsPIPs had two conserved NPA motifs except for PsPIP1-1, PsPIP2-2-1, and PsPIP2-3, each having a single NPA motif. Among PsNIPs, PsNIP1-6, PsNIP1-6, PsNIP1-7, PsNIP3-1, PsNIP4-1 and PSNIP4-2 had two NPA domains, while PsNIP1-1, PsNIP2-1-2, PsNIP2-2-2 and PsNIP6-1 each had a single NPA motif. In the PsNIP sub-family, the first NPA motif showed an Alanine (A) to Valine (V) substitution in three PsNIPs (PsNIP1-3, PsNIP1-5, and PsNIP6-3) (Table 2). Furthermore, the NPA domains of all members of the XIP and SIP subfamilies were different. The second NPA motif was conserved in PsSIP aquaporins, however, all of the first NPA motifs had Alanine (A) replaced by Leucine (L) (PsSIP2-1-1, PsSIP2-1-2) or Threonine (T) (PsSIP1-1). In comparison to other subfamilies, this motif variation distinguishes water and solute-transporting aquaporins[45].

Compared to NPA motifs, the ar/R positions were more variable and the amino acid composition appeared to be subfamily-dependent. The majority of PsPIPs had phenylalanine at H2, histidine at H5, threonine at LE1, and arginine at LE2 selective filter (Table 2). All of the PsTIP1 members had a Histidine-Isoleucine-Alanine-Valine structure at this position, while all PsTIP2 members but PsTIP2-3 harbored Histidine-Isoleucine-Glycine-Arginine. Similarly, PsNIPs, PsSIPs and PsXIP also showed subgroup-specific variation in ar/R selectivity filter (Table 2). Each of these substitutions partly determines the function of transporting water[46].

**Table 1.** Description and distribution of aquaporin genes identified in the garden pea genome.

| | | | | Chromosome | | | | | |
|---|---|---|---|---|---|---|---|---|---|
| S. No | Gene Name | Gene ID | Gene length (bp) | Location | Start | End | Transcription length (bp) | CDS length (bp) | Protein length (aa) |
| 1 | *PsPIP1-1* | Psat5g128840.3 | 2507 | chr5LG3 | 231,127,859 | 231,130,365 | 675 | 675 | 225 |
| 2 | *PsPIP1-2* | Psat2g034560.1 | 1963 | chr2LG1 | 49,355,958 | 49,357,920 | 870 | 870 | 290 |
| 3 | *PsPIP1-4* | Psat2g182480.1 | 1211 | chr2LG1 | 421,647,518 | 421,648,728 | 864 | 864 | 288 |
| 4 | *PsPIP2-1* | Psat6g183960.1 | 3314 | chr6LG2 | 369,699,084 | 369,702,397 | 864 | 864 | 288 |
| 5 | *PsPIP2-2-1* | Psat4g051960.1 | 1223 | chr4LG4 | 86,037,446 | 86,038,668 | 585 | 585 | 195 |
| 6 | *PsPIP2-2-2* | Psat5g279360.2 | 2556 | chr5LG3 | 543,477,849 | 543,480,404 | 2555 | 789 | 263 |
| 7 | *PsPIP2-3* | Psat7g228600.2 | 2331 | chr7LG7 | 458,647,213 | 458,649,543 | 2330 | 672 | 224 |
| 8 | *PsPIP2-4* | Psat3g045080.1 | 1786 | chr3LG5 | 100,017,377 | 100,019,162 | 864 | 864 | 288 |
| 9 | *PsPIP2-5* | Psat0s3550g0040.1 | 1709 | scaffold03550 | 20,929 | 22,637 | 1191 | 1191 | 397 |
| 10 | *PsTIP1-1* | Psat3g040640.1 | 2021 | chr3LG5 | 89,426,473 | 89,428,493 | 753 | 753 | 251 |
| 11 | *PsTIP1-3* | Psat3g184440.1 | 2003 | chr3LG5 | 393,920,756 | 393,922,758 | 759 | 759 | 253 |
| 12 | *PsTIP1-4* | Psat7g219600.1 | 2083 | chr7LG7 | 441,691,937 | 441,694,019 | 759 | 759 | 253 |
| 13 | *PsTIP1-7* | Psat6g236600.1 | 1880 | chr6LG2 | 471,659,417 | 471,661,296 | 762 | 762 | 254 |
| 14 | *PsTIP2-1* | Psat1g005320.1 | 1598 | chr1LG6 | 7,864,810 | 7,866,407 | 750 | 750 | 250 |
| 15 | *PsTIP2-2* | Psat4g198360.1 | 1868 | chr4LG4 | 407,970,525 | 407,972,392 | 750 | 750 | 250 |
| 16 | *PsTIP2-3* | Psat1g118120.1 | 2665 | chr1LG6 | 230,725,833 | 230,728,497 | 768 | 768 | 256 |
| 17 | *PsTIP2-6* | Psat2g177040.1 | 1658 | chr2LG1 | 416,640,482 | 416,642,139 | 750 | 750 | 250 |
| 18 | *PsTIP3-2* | Psat6g054400.1 | 1332 | chr6LG2 | 54,878,003 | 54,879,334 | 780 | 780 | 260 |
| 19 | *PsTIP4-1* | Psat6g037720.2 | 1689 | chr6LG2 | 30,753,624 | 30,755,312 | 1688 | 624 | 208 |
| 20 | *PsTIP5-1* | Psat7g157600.1 | 1695 | chr7LG7 | 299,716,873 | 299,718,567 | 762 | 762 | 254 |
| 21 | *PsNIP1-1* | Psat1g195040.2 | 1864 | chr1LG6 | 346,593,853 | 346,595,716 | 1863 | 645 | 215 |
| 22 | *PsNIP1-3* | Psat1g195800.1 | 1200 | chr1LG6 | 347,120,121 | 347,121,335 | 819 | 819 | 273 |
| 23 | *PsNIP1-5* | Psat7g067480.1 | 2365 | chr7LG7 | 109,420,633 | 109,422,997 | 828 | 828 | 276 |
| 24 | *PsNIP1-6* | Psat7g067360.1 | 2250 | chr7LG7 | 109,270,462 | 109,272,711 | 813 | 813 | 271 |
| 25 | *PsNIP1-7* | Psat1g193240.1 | 1452 | chr1LG6 | 344,622,606 | 344,624,057 | 831 | 831 | 277 |
| 26 | *PsNIP2-1-2* | Psat3g197520.1 | 669 | chr3LG5 | 420,092,382 | 420,093,050 | 345 | 345 | 115 |
| 27 | *PsNIP2-2-2* | Psat3g197560.1 | 716 | chr3LG5 | 420,103,168 | 420,103,883 | 486 | 486 | 162 |
| 28 | *PsNIP3-1* | Psat2g072000.1 | 1414 | chr2LG1 | 133,902,470 | 133,903,883 | 798 | 798 | 266 |
| 29 | *PsNIP4-1* | Psat7g126440.1 | 1849 | chr7LG7 | 209,087,362 | 209,089,210 | 828 | 828 | 276 |
| 30 | *PsNIP4-2* | Psat5g230920.1 | 1436 | chr5LG3 | 463,340,575 | 463,342,010 | 825 | 825 | 275 |
| 31 | *PsNIP5-1* | Psat6g190560.1 | 1563 | chr6LG2 | 383,057,323 | 383,058,885 | 867 | 867 | 289 |
| 32 | *PsNIP6-1* | Psat5g304760.4 | 5093 | chr5LG3 | 573,714,868 | 573,719,960 | 5092 | 486 | 162 |
| 33 | *PsNIP6-2* | Psat7g036680.1 | 2186 | chr7LG7 | 61,445,341 | 61,447,134 | 762 | 762 | 254 |
| 34 | *PsNIP6-3* | Psat7g259640.1 | 2339 | chr7LG7 | 488,047,315 | 488,049,653 | 918 | 918 | 306 |
| 35 | *PsNIP7-1* | Psat6g134160.2 | 4050 | chr6LG2 | 260,615,019 | 260,619,068 | 4049 | 1509 | 503 |
| 36 | *PsSIP1-1* | Psat3g091120.1 | 3513 | chr3LG5 | 187,012,329 | 187,015,841 | 738 | 738 | 246 |
| 37 | *PsSIP1-2* | Psat1g096840.1 | 3609 | chr1LG6 | 167,126,599 | 167,130,207 | 744 | 744 | 248 |
| 38 | *PsSIP1-3* | Psat7g203280.1 | 2069 | chr7LG7 | 401,302,247 | 401,304,315 | 720 | 720 | 240 |
| 39 | *PsSIP2-1-1* | Psat0s2987g0040.1 | 706 | scaffold02987 | 177,538 | 178,243 | 621 | 621 | 207 |
| 40 | *PsSIP2-1-2* | Psat3g082760.1 | 3135 | chr3LG5 | 173,720,100 | 173,723,234 | 720 | 720 | 240 |
| 41 | *PsXIP2-1* | Psat7g178080.1 | 2077 | chr7LG7 | 335,167,251 | 335,169,327 | 942 | 942 | 314 |

bp: base pair, aa: amino acid.

## Predicted subcellular localization of PsAQPs

Sequence-based subcellular localization analysis using WoLF PSORT predicted that all PsPIPs localized in the plasma membrane, which is consistent with their subfamily classification (Table 2). Around half (5/11) of the PsTIPs (PsTIP1-4, PsTIP2-1, PsTIP2-6, PsTIP4-1, and PsTIP5-1) were predicted to localize within vacuoles. However, several TIP members (PsTIP1-1, PsTIP1-3, PsTIP1-7, PsTIP2-2, PsTIP2-3 and PsTIP3-2) were predicted to localize in plasma membranes. We then further investigated their localizations by using another software (Plant-mPLoc, Table 2), which predicted that all the PsTIPs localize within vacuoles, thus supporting that they are tonoplast related. An overwhelming majority of PsNIPs (14/15) and PsXIP were predicted to be found only in plasma membranes., which was also expected (Table 2). Collectively, the versatility in subcellular localization of the pea AQPs is implicative of their distinct roles in controlling water and/or solute transport in the context of plant cell compartmentation.

## Tissue expression profiles of PsAQPs

Tissue expression patterns of genes are indicative of their functions. Since there were rich resources of RNA-Seq data from various types of pea tissues in the public database, they were used for the extraction of expression information of *PsAQP* genes as represented by FPKM values. A heat map was generated to show the expression patterns of *PsAQP* genes in 18 different tissues/stages and their responses to nitrate levels (Fig. 4). According to the heat map, *PsPIP1-2*, *PsPIP2-3* were highly expressed in root and nodule G (Low-nitrate), whereas *PsTIP1-4*, *PsTIP2-6*, and *PsNIP1-7* were only expressed in roots in comparison to other tissues. The result also demonstrated that *PsPIP1-1* and *PsNIP3-1* expressed more abundantly in leaf, tendril, and peduncle, whereas *PsPIP2-2-2* and *PsTIP1-1* showed

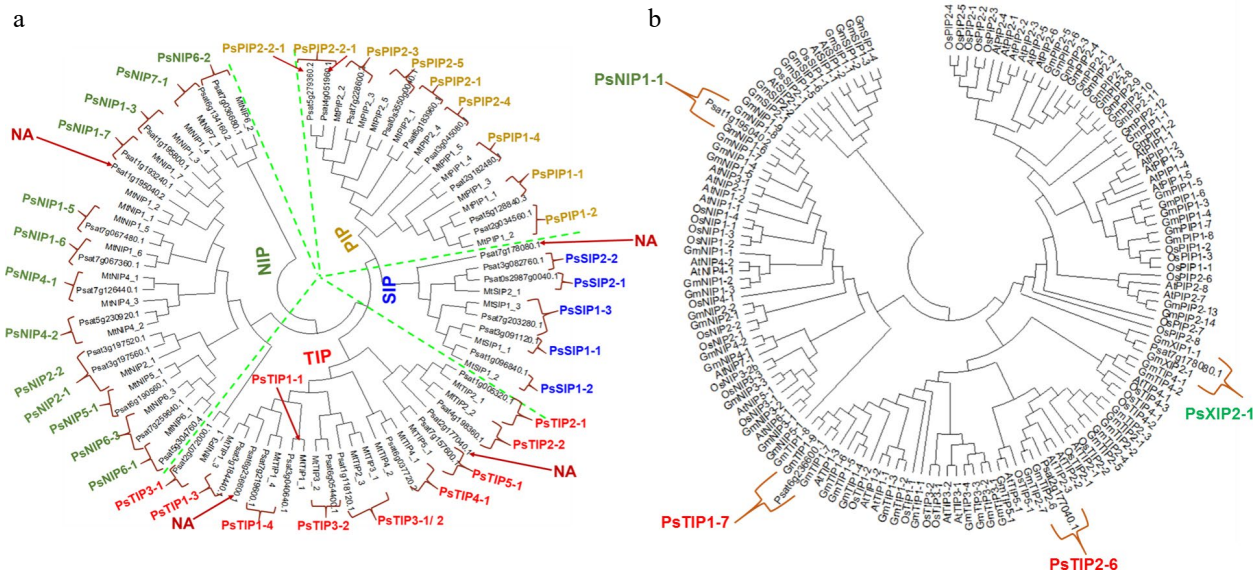


**Fig. 1** Phylogenetic analysis of the identified AQPs from pea genome. (a) The pea AQPs proteins aligned with those from the cool-season legume *Medicago truncatual*. (b) The four un-assigned pea AQPs in (a) (denoted as NA) were further aligned with the AQPs of rice, soybean, and Arabidopsis by using the Clustal W program implemented in MEGA 7 software. The nomenclature of PsAQPs was based on homology with the identified aquaporins that were clustered together.

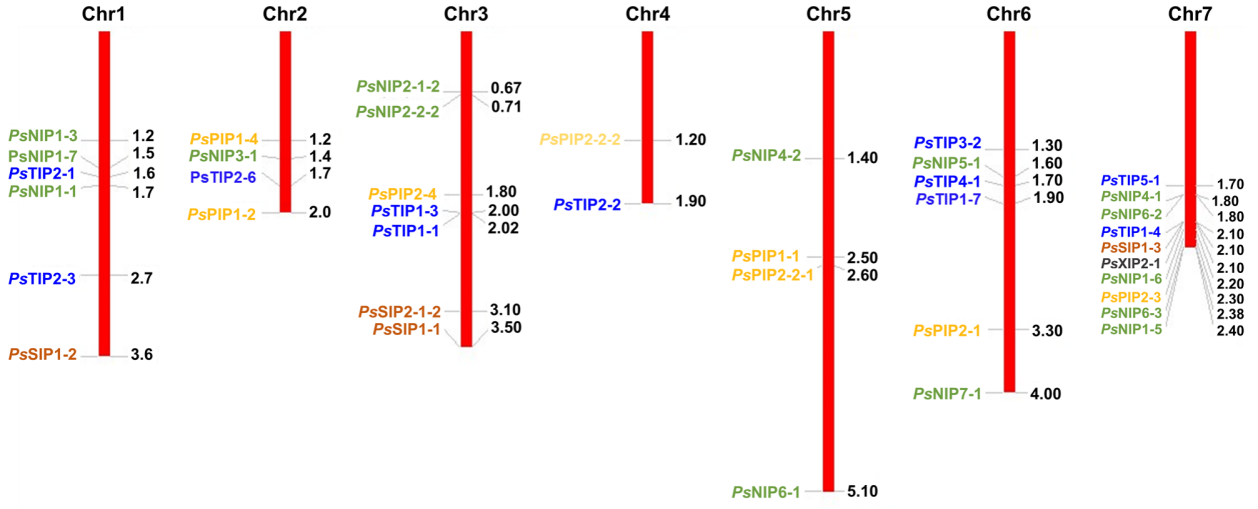


**Fig. 2** Chromosomal localization of the 41 *PsAQPs* on the seven chromosomes of pea. Chr1-7 represents the chromosomes 1 to 7. The numbers on the right of each chromosome show the physical map positions of the AQP genes (Mbp). Blue, green, orange, brown, and black colors represent TIPs, NIPs, PIPs, SIPs, and XIP, respectively.

high to moderate expressions in all the samples except for a few. Interestingly, *PsTIP1-1* expression in many green tissues seemed to be oppressed by low-nitrate. In contrast, some AQPs such as *PsTIP1-3*, *PsTIP1-7*, *PsTIP5-1*, *PsNIP1-5*, *PsNIP4-1*, *PsNIP5-1*, and *PsSIP2-1-1* showed higher expression only in the flower tissue. There were interesting developmental stage-dependent regulations of some AQPs in seeds (Fig. 4). For example, *PsPIP2-1*, *PsPIP2-2-1*, *PsNIP1-6*, *PsSIP1-1*, and *PsSIP1-2* were more abundantly expressed in the Seed_12 dap (days after pollination;) tissue than in the Seed_5 dai (days after imbibition) tissue; reversely, *PsPIP2-2-2*, *PsPIP2-4*, *PsTIP2-3*, and *PsTIP3-2* showed higher expression in seed_5 dai in compare to seed_12 dap tissues (Fig. 4). The AQP genes may have particular functional roles in the growth and development of the pea based on their tissue-specific expression.

## PsAQPs expressions in response to osmotic stress and fullerol treatment in imbibing embryos

Expressions of plant *AQPs* in vegetative tissues under normal and stressed conditions have been extensively studied[15]; however, little is known about the transcriptional regulation of *AQP* genes in seeds/embryos. To provide insights into this specific area, wet-bench RNA-Seq was performed on the germinating embryo samples isolated from water (W)-imbibed seeds and those treated with mannitol (M, an osmotic reagent), mannitol, and mannitol plus fullerol (F, a nano-antioxidant). The phenotypic evaluation showed that M treatment had a substantial inhibitory effect on radicle growth, whereas the supplement of F significantly mitigated this inhibition at all concentrations, in particular, 100 mg/mL in MF3, which increased the radicle length by ~33% as compared to that

**Table 2.** Protein information, conserved amino acid residues, trans-membrane domains, selectivity filter, and predicted subcellular localization of the 39 full-length pea aquaporins.

| S. No | AQPs | Gene | Length | TMH | NPA | NPA | ar/R selectivity filter | | | | pI | WoLF PSORT | Plant-mPLoc |
|---|---|---|---|---|---|---|---|---|---|---|---|---|---|
| | | | | | LB | LE | H2 | H5 | LE1 | LE2 | | | |
| Plasma membrane intrinsic proteins (PIPs) | | | | | | | | | | | | | |
| 1 | PsPIP1-1 | Psat5g128840.3 | 225 | 4 | NPA | 0 | F | 0 | 0 | 0 | 8.11 | Plas | Plas |
| 2 | PsPIP1-2 | Psat2g034560.1 | 290 | 2 | NPA | NPA | F | H | T | R | 9.31 | Plas | Plas |
| 3 | PsPIP1-4 | Psat2g182480.1 | 288 | 6 | NPA | NPA | F | H | T | R | 9.29 | Plas | Plas |
| 4 | PsPIP2-1 | Psat6g183960.1 | 288 | 6 | NPA | NPA | F | H | T | 0 | 8.74 | Plas | Plas |
| 5 | PsPIP2-2-1 | Psat4g051960.1 | 195 | 3 | 0 | 0 | F | H | T | R | 8.88 | Plas | Plas |
| 6 | PsPIP2-2-2 | Psat5g279360.2 | 263 | 5 | NPA | NPA | F | H | T | R | 5.71 | Plas | Plas |
| 7 | PsPIP2-3 | Psat7g228600.2 | 224 | 4 | NPA | 0 | F | F | 0 | 0 | 6.92 | Plas | Plas |
| 8 | PsPIP2-4 | Psat3g045080.1 | 288 | 6 | NPA | NPA | F | H | T | R | 8.29 | Plas | Plas |
| Tonoplast intrinsic proteins (TIPs) | | | | | | | | | | | | | |
| 1 | PsTIP1-1 | Psat3g040640.1 | 251 | 7 | NPA | NPA | H | I | A | V | 6.34 | Plas | Vacu |
| 2 | PsTIP1-3 | Psat3g184440.1 | 253 | 6 | NPA | NPA | H | I | A | V | 5.02 | Plas/Vacu | Vacu |
| 3 | PsTIP1-4 | Psat7g219600.1 | 253 | 7 | NPA | NPA | H | I | A | V | 4.72 | Vacu | Vacu |
| 4 | PsTIP1-7 | Psat6g236600.1 | 254 | 6 | NPA | NPA | H | I | A | V | 5.48 | Plas/Vacu | Vacu |
| 5 | PsTIP2-1 | Psat1g005320.1 | 250 | 6 | NPA | NPA | H | I | G | R | 8.08 | Vacu | Vacu |
| 6 | PsTIP2-2 | Psat4g198360.1 | 250 | 6 | NPA | NPA | H | I | G | R | 5.94 | Plas/Vacu | Vacu |
| 7 | PsTIP2-3 | Psat1g118120.1 | 256 | 6 | NPA | NPA | H | I | A | L | 6.86 | Plas/Vacu | Vacu |
| 8 | PsTIP2-6 | Psat2g177040.1 | 250 | 6 | NPA | NPA | H | I | G | R | 4.93 | Vacu | Vacu |
| 9 | PsTIP3-2 | Psat6g054400.1 | 260 | 6 | NPA | NPA | H | I | A | R | 7.27 | Plas/Vacu | Vacu |
| 10 | PsTIP4-1 | Psat6g037720.2 | 208 | 6 | NPA | NPA | H | I | A | R | 6.29 | Vac/ plas | Vacu |
| 11 | PsTIP5-1 | Psat7g157600.1 | 254 | 7 | NPA | NPA | N | V | G | C | 8.2 | Vacu /plas | Vacu/Plas |
| Nodulin-26 like intrisic proteins (NIPs) | | | | | | | | | | | | | |
| 1 | PsNIP1-1 | Psat1g195040.2 | 215 | 5 | NPA | 0 | W | V | F | 0 | 6.71 | Plas | Plas |
| 2 | PsNIP1-3 | Psat1g195800.1 | 273 | 5 | NPA | NPV | W | V | A | R | 6.77 | Plas | Plas |
| 3 | PsNIP1-5 | Psat7g067480.1 | 276 | 6 | NPA | NPV | W | V | A | N | 8.98 | Plas | Plas |
| 4 | PsNIP1-6 | Psat7g067360.1 | 271 | 6 | NPA | NPA | W | V | A | R | 8.65 | Plas/Vacu | Plas |
| 5 | PsNIP1-7 | Psat1g193240.1 | 277 | 6 | NPA | NPA | W | I | A | R | 6.5 | Plas/Vacu | Plas |
| 6 | PsNIP2-1-2 | Psat3g197520.1 | 115 | 2 | NPA | O | G | 0 | 0 | 0 | 9.64 | Plas | Plas |
| 7 | PsNIP2-2-2 | Psat3g197560.1 | 162 | 3 | 0 | NPA | 0 | S | G | R | 6.51 | Plas | Plas |
| 8 | PsNIP3-1 | Psat2g072000.1 | 266 | 5 | NPA | NPA | S | I | A | R | 8.59 | Plas/Vacu | Plas |
| 9 | PsNIP4-1 | Psat7g126440.1 | 276 | 6 | NPA | NPA | W | V | A | R | 6.67 | Plas | Plas |
| 10 | PsNIP4-2 | Psat5g230920.1 | 275 | 6 | NPA | NPA | W | L | A | R | 7.01 | Plas | Plas |
| 11 | PsNIP5-1 | Psat6g190560.1 | 289 | 5 | NPS | NPV | A | I | G | R | 7.1 | Plas | Plas |
| 12 | PsNIP6-1 | Psat5g304760.4 | 162 | 2 | NPA | 0 | I | 0 | 0 | 0 | 9.03 | Plas | Plas |
| 13 | PsNIP6-2 | Psat7g036680.1 | 254 | 0 | 0 | 0 | G | 0 | 0 | 0 | 5.27 | Chlo | Plas/Nucl |
| 14 | PsNIP6-3 | Psat7g259640.1 | 306 | 6 | NPA | NPV | T | I | G | R | 8.32 | Plas | Plas |
| 15 | PsNIP7-1 | Psat6g134160.2 | 503 | 0 | NLK | 0 | W | G | Q | R | 8.5 | Vacu | Chlo/Nucl |
| Small basic intrinsic proteins (SIPs) | | | | | | | | | | | | | |
| 1 | PsSIP1-1 | Psat3g091120.1 | 246 | 6 | NPT | NPA | V | L | P | N | 9.54 | Plas | Plas/Vacu |
| 2 | PsSIP1-2 | Psat1g096840.1 | 248 | 5 | NTP | NPA | I | V | P | L | 9.24 | Vacu | Plas/Vacu |
| 3 | PsSIP1-3 | Psat7g203280.1 | 240 | 6 | NPS | NPA | N | L | P | N | 10.32 | Chlo | Plas |
| 4 | PsSIP2-1-2 | Psat3g082760.1 | 240 | 4 | NPL | NPA | Y | L | G | S | 10.28 | Plas | Plas |
| Uncharacterized X intrinsic proteins (XIPs) | | | | | | | | | | | | | |
| 1 | PsXIP2-1 | Psat7g178080.1 | 314 | 6 | SPV | NPA | V | V | R | M | 7.89 | Plas | Plas |

Length: protein length (aa); pI: Isoelectric point; Trans-membrane helicase (TMH) represents for the numbers of Trans-membrane helices predicted by *TMHMM Server v.2.0 tool*; WoLF PSORT and Plant-mPLoc: best possible cellualr localization predicted by the WoLF PSORT and Plant-mPLoc tool, respectively (*Chlo* Chloroplast, *Plas* Plasma membrane, *Vacu* Vacuolar membrane, *Nucl* Nucleus); LB: Loop B, L: Loop E; NPA: Asparagine-Proline-Alanine; H2 represents for Helix 2, H5 represents for Helix 5, LE1 represents for Loop E1, LE2 represents for Loop E2, Ar/R represents for Aromatic/Arginine.

under solely M treatment (Fig. 5). The expression values of *PsAQP* genes were removed from the RNA-Seq data, and pairwise comparisons were made within the Group 1: W *vs* M, and Group 2: W *vs* MF3, where a total of ten and nince *AQPs* were identified as differentially expressed genes (DEGs), respectively (Fig. 6). In Group 1, six DEGs were up-regulated and four DEGs down-regulated, whereas in Group 2, six DEGs were up-regulated and three DEGs down-regulated. Four genes viz. *PsPIPs2-5*, *PsNIP6-3*, *PsTIP2-3*, and *PsTIP3-2* were found to be similarly regulated by M or MF3 treatment (Fig. 6), indicating that their regulation by osmotic stress couldn't be mitigated by fullerol. Three genes, all being *PsNIPs* (1-1, 2-1-2, and 4-2), were up-regulated only under mannitol treatment without fullerol, suggesting that their perturbations by osmotic stress were migrated by the antioxidant activities. In contrast, four other genes namely *PsTIP2-2*, *PsTIP4-1*, *PsNIP1-5*, and *PsSIP1-3* were only regulated under mannitol treatment when fullerol was present.

## Validation of the DEGs through qRT-PCR

As a validation of the RNA-Seq data, eight genes showing differential expressions in imbibing seeds under M or M + F treatments were selected for qRT-PCR analysis, which was

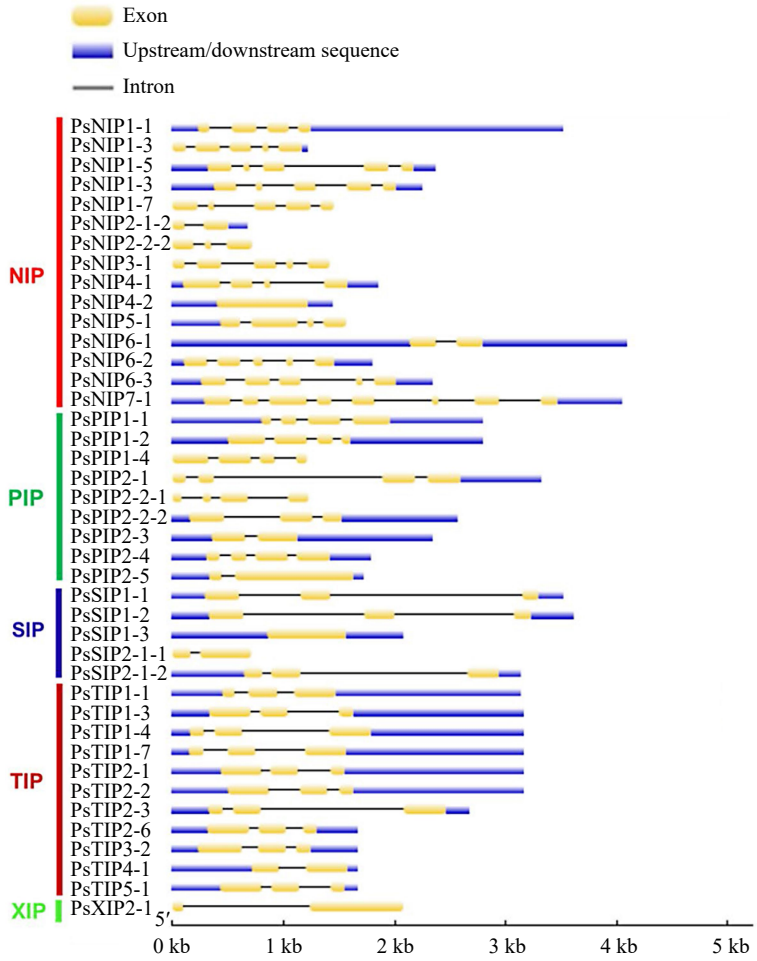


**Fig. 3** The exon-intron structures of the *AQP* genes in pea. Upstream/downstream region, exon, and intron are represented by a blue box, yellow box, and grey line, respectively.

*PsTIP4-1*, *PsTIP2-2*, *PsTIP2-3*, *PsTIP3-2*, *PsPIP2-5*, P*sXIP2-1*, *PsNIP6-3* and *PsNIP1-5* shown in Fig 6, the expression modes of all the selected genes but *PsXIP2-1* were well consistent between the RNA-Seq and the qRT-PCR data. *PsXIP2-1*, exhibiting slightly decreased expression under M treatment according to RNA-Seq, was found to be up-regulated under the same treatment by qRT-PCR (Fig. 7). This gene was therefore removed from further discussions.

## DISCUSSION

This study used the recently available garden pea genome to perform genome-wide identification of AQPs[35] to help understand their functions in plant growth and development. A total of 39 putative full-length AQPs were found in the garden pea genome, which is very similar to the number of AQPs identified in many other diploid legume crops such as 40 AQPs genes in pigeon pea, chickpea, common bean[7,47,48], and 44 AQPs in Medicago[49]. On the other hand, the number of AQP genes in pea is greater compared to diploid species like rice (34)[4], *Arabidopsis thaliana* (35)[3], and 32 and 36 in peanut A and B genomes, respectively[8]. Phylogenetic analysis assigned the pea AQPs into all five subfamilies known in plants, whereas the presence of only one XIP in this species seems less than the number in other diploid legumes which have two each in common bean and Medicago[5,48,49]. The functions of the XIP-type AQP will be of particular interest to explore in the future.

The observed exon-intron structures in pea AQPs were found to be conserved and their phylogenetic distribution often correlated with these structures. Similar exon-intron patterns were seen in PIPs and TIPs subfamily of Arabidopsis, soybean, and tomato[3,6,50]. The two conserved NPA motifs and the four amino acids forming the ar/R SF mostly regulate solute specificity and transport of the substrate across AQPs[47,51]. According to our analysis, all the members of each AQP subfamilies in garden pea showed mostly conserved NPA motifs and a similar ar/R selective filter. Interestingly, most PsPIPs carry double NPA in LB and LE and a hydrophilic ar/R SF (F/H/T/R) as observed in three legumes i.e., common bean[48], soybean[5] chickpea[7], showing their affinity for water transport. All the TIPs of garden pea have double NPA in LB and LE and wide variation at selectivity filters. Most PsTIP1s (1-1, 1-3, 1-4, and 1-7) were found with H-I-A-V ar/R selectivity filter similar to other species such as Medicago, Arachis, and common bean, that are reported to transport water and other small molecules like boron, hydrogen peroxide, urea, and ammonia[52]. Compared with related species, the TIPs residues in the ar/R selectivity filter were very similar to those in

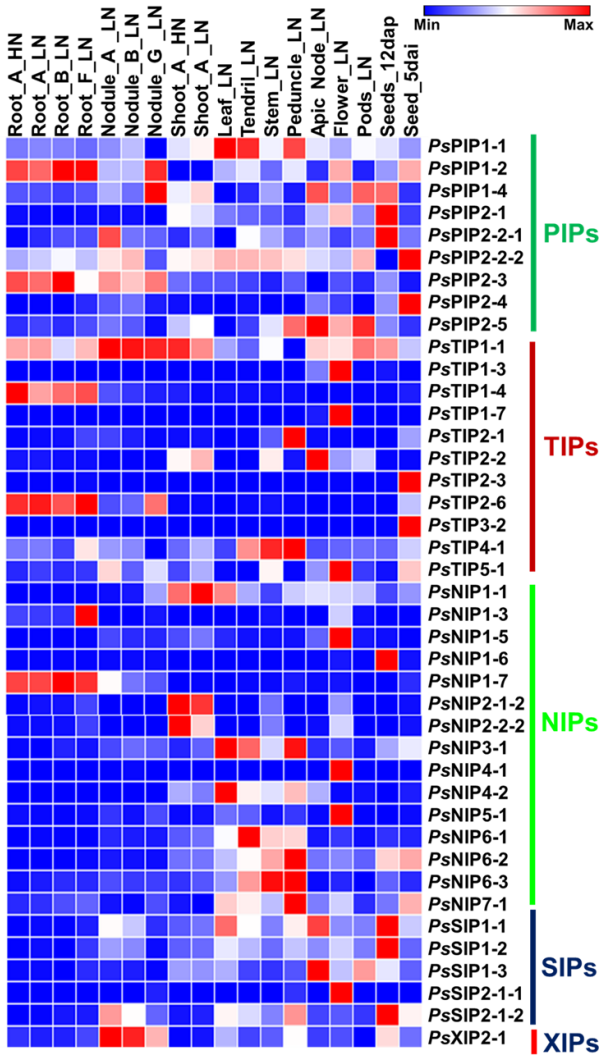


**Fig. 4** Heatmap analysis of the expression of pea *AQP* gene expressions in different tissues using RNA-seq data (PRJNA267198). Normalized expression of aquaporins in terms of reads per kilobase of transcript per million mapped reads (RPKM) showing higher levels of PIPs, NIPs, TIPs SIPs, and XIP expression across the different tissues analyzed. (Stage A represents 7-8 nodes; stage B represents the start of flowering; stage D represents germination, 5 d after imbibition; stage E represents 12 d after pollination; stage F represents 8 d after sowing; stage G represents 18 d after sowing, LN: Low-nitrate; HN: High-nitrate.

common bean[48], Medicago[49], and Arachis[8]. In the present study, the NIPs, NIP1s (1-3, 1-5, 1-6, and1-7), and NIP2-2-2 genes have G-S-G-R selectivity. Interestingly, NIP2s with a G-S-G-R selectivity filter plays an important role in silicon influx (Si) in many plant species such as Soybean and Arachis[6,8]. It was reported that Si accumulation protects plants against various types of biotic and abiotic stresses[53].

The subcellular localization investigation suggested that most of the PsAQPs were localized to the plasma membrane or vacuolar membrane. The members of the PsPIPs, PsNIPs, and PsXIP subfamilies were mostly located in the plasma membrane, whereas members of the PsTIPs subfamily were often predicted to localize in the vacuolar membrane. Similar situations were reported in many other legumes such as common bean, soybean, and chickpea[5,7,48]. Apart from that, PsSIPs subfamily were predicted to localize to the plasma membrane or vacuolar membrane, and some AQPs were likely to localize in broader subcellular positions such as the nucleus, cytosol, and chloroplast, which indicates that AQPs may be involved in various molecular transport functions.

AQPs have versatile physiological functions in various plant organs. Analysis of RNA-Seq data showed a moderate to high expression of the *PsPIPs* in either root or green tissues except for *PsPIP2-4*, indicating their affinity to water transport. In several other species such as Arachis[8], common bean[48], and Medicago[49], PIPs also were reported to show high expressions and were considered to play an important role to maintain root and leaf hydraulics. Also interestingly, *PsTIP2-3* and *PsTIP3-2* showed high expressions exclusively in seeds at 5 d after imbibition, indicating their specific roles in seed germination. Earlier, a similar expression pattern for *TIP3s* was reported in Arabidopsis during the initial phase of seed germination and seed maturation[54], soybean[6], canola[55], and Medicago[49], suggesting that the main role of TIP3s in regulating seed development is conserved across species.

Carbon nanoparticles such as fullerol have a wide range of potential applications as well as safety concerns in agriculture. Fullerol has been linked to plant protection from oxidative stress by influencing ROS accumulation and activating the antioxidant system in response to drought[56]. The current study revealed that fullerol at an adequate concentration (100 mg/L), had favorable effects on osmotic stress alleviation. In this study, the radical growth of germinating seeds was repressed by the mannitol treatment, and many similar observations have been found in previous studies[57]. Furthermore, mannitol induces ROS accumulation in plants, causing oxidative stress[58]. Our work further validated that the radical growth of germinating seeds were increased during fullerol treatment. Fullerol increased the length of roots and barley seeds, according to Panova et al.[32]. Fullerol resulted in ROS detoxification in seedlings subjected to water stress[32].

Through transcriptomic profiling and qRT-PCR, several *PsAQPs* that responded to osmotic stress by mannitol and a combination of mannitol and fullerol were identified. Most of these differentially expressed *AQPs* belonged to the *TIP* and *NIP* subfamilies. (PsTIP2-2, PsTIP2-3, and PsTIP 3-2) showed higher expression by mannitol treatment, which is consistent with the fact that many *TIPs* in other species such as *GmTIP2;3* and *Eucalyptus grandis TIP2* (*EgTIP2*) also showed elevated expressions under osmotic stress[54,59]. The maturation of the vacuolar apparatus is known to be aided by the TIPs, which also enable the best possible water absorption throughout the growth of embryos and the germination of seeds[60]. Here, the higher expression of *PsTIP* (2-2, 2-3, and 3-2) might help combat water deficiency in imbibing seeds due to osmotic stress. The cellular signals triggering such transcriptional regulation seem to be independent of the antioxidant system because the addition of fullerol didn't remove such regulation. On the other hand, the mannitol-induced regulation of most *PsNIPs* were eliminated when fullerol was added, suggesting either a response of these *NIPs* to the antioxidant signals or being due to the mitigated cellular stress. Based on our experimental data and previous knowledge, we propose that the fullerol-induced up- or down-regulation of specific *AQPs* belonging to different

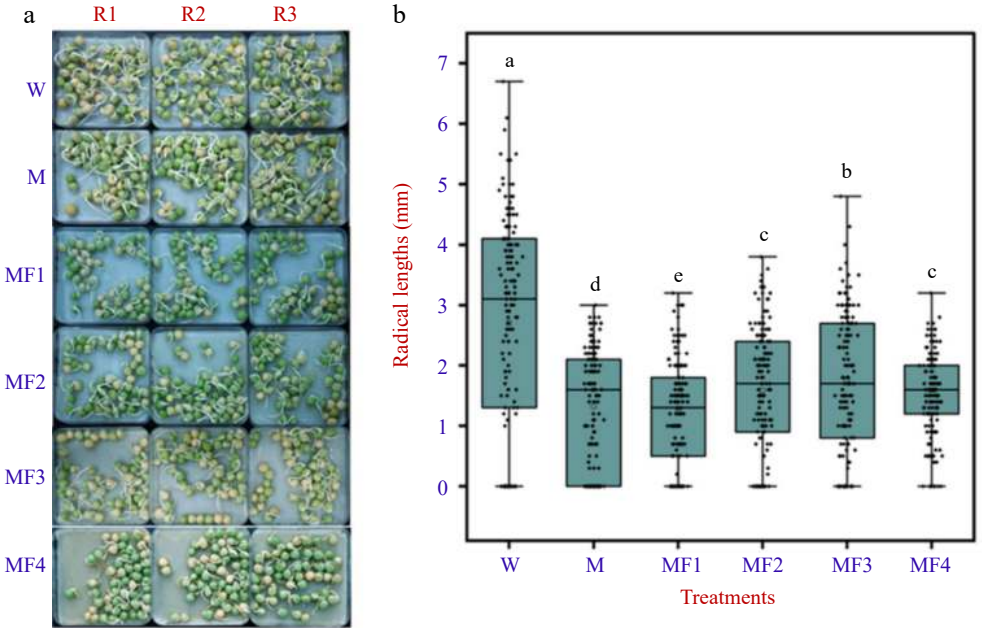


**Fig. 5** The visual phenotype and radicle length of pea seeds treated with water (W), 0.3 M mannitol (M), and fullerol of different concentrations dissolved in 0.3 M mannitol (MF). MF1, MF2, MF3, and MF4 indicated fullerol dissolved in 0.3 M mannitol at the concentration of 10, 50, 100, and 500 mg/L, respectively. (a) One hundred and fifty grains of pea seeds each were used for phenotype analysis at 72 h after treatment. Radicle lengths were measured using a ruler in three replicates R1, R2, and R3 in all the treatments. (b) Multiple comparison results determined using the SSR-Test method were shown with lowercase letters to indicate statistical significance ($P < 0.05$).

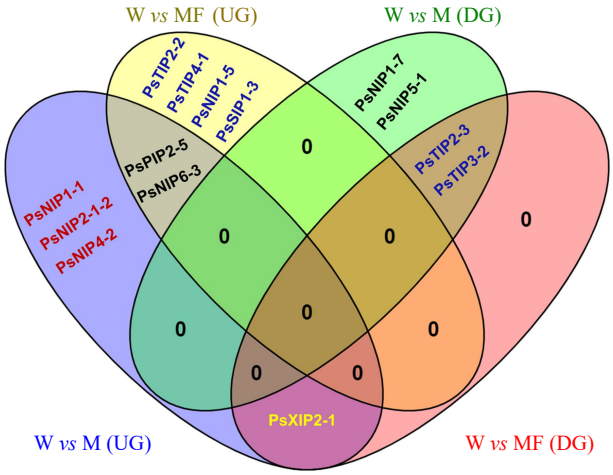


**Fig. 6** Venn diagram showing the shared and unique differentially expressed *PsAQP* genes in imbibing seeds under control (W), Mannitol (M) and Mannitol + Fullerol (MF3) treatments. Up-regulation (UG): PsPIP2-5, PsNIP1-1, PsNIP2-1-2, PsNIP4-2, PsNIP6-3, PsNIP1-5, PsTIP2-2, PsTIP4-1, PsSIP1-3, PsXIP2-1; Down-regulation (DG): PsTIP2-3, PsTIP3-2, PsNIP1-7, PsNIP5-1, PsXIP2-1.

subfamilies and locating in different subcellular compartments, work coordinatedly with each other, to maintain the water balance and strengthen the tolerance to osmotic stress in germinating pea seeds through reduction of ROS accumulation and enhancement of antioxidant enzyme levels. Uncategorized X intrinsic proteins (XIPs) Aquaporins are multifunctional channels that are accessible to water, metalloids, and ROS.[32,56]. Due likely to PCR bias, the expression data of *PsXIP2-1* from qRT-PCR and RNA-Seq analyses didn't match well, hampering the drawing of a solid conclusion about this gene. Further studies are required to verify and more deeply dissect the functions of each of these *PsAQPs* in osmotic stress tolerance.

## CONCLUSIONS

A total of 39 full-length *AQP* genes belonging to five subfamilies were identified from the pea genome and characterized for their sequences, phylogenetic relationships, gene structures, subcellular localization, and expression profiles. The number of *AQP* genes in pea is similar to that in related diploid legume species. The RNA-seq data revealed that *PsTIP* (2-3, 3-2) showed high expression in seeds for 5 d after imbibition, indicating their possible role during the initial phase of seed germination. Furthermore, gene expression profiles displayed that higher expression of *PsTIP* (2-3, 3-2) in germinating seeds might help maintain water balance under osmotic stress to confer tolerance. Our results suggests that the biological functions of fullerol in plant cells are exerted partly through the interaction with AQPs.

### Deposition of raw data

Under Bio project ID PRJNA793376 at the National Center for Biotechnology Information, raw data of sequencing read has been submitted. The accession numbers for the RNA-seq raw data are stored in GenBank and are mentioned in Supplemental Table S4.

## ACKNOWLEDGMENTS

This study is supported by the National Key Research & Development Program of China (2022YFE0198000) and the Key Research Program of Zhejiang Province (2021C02041).

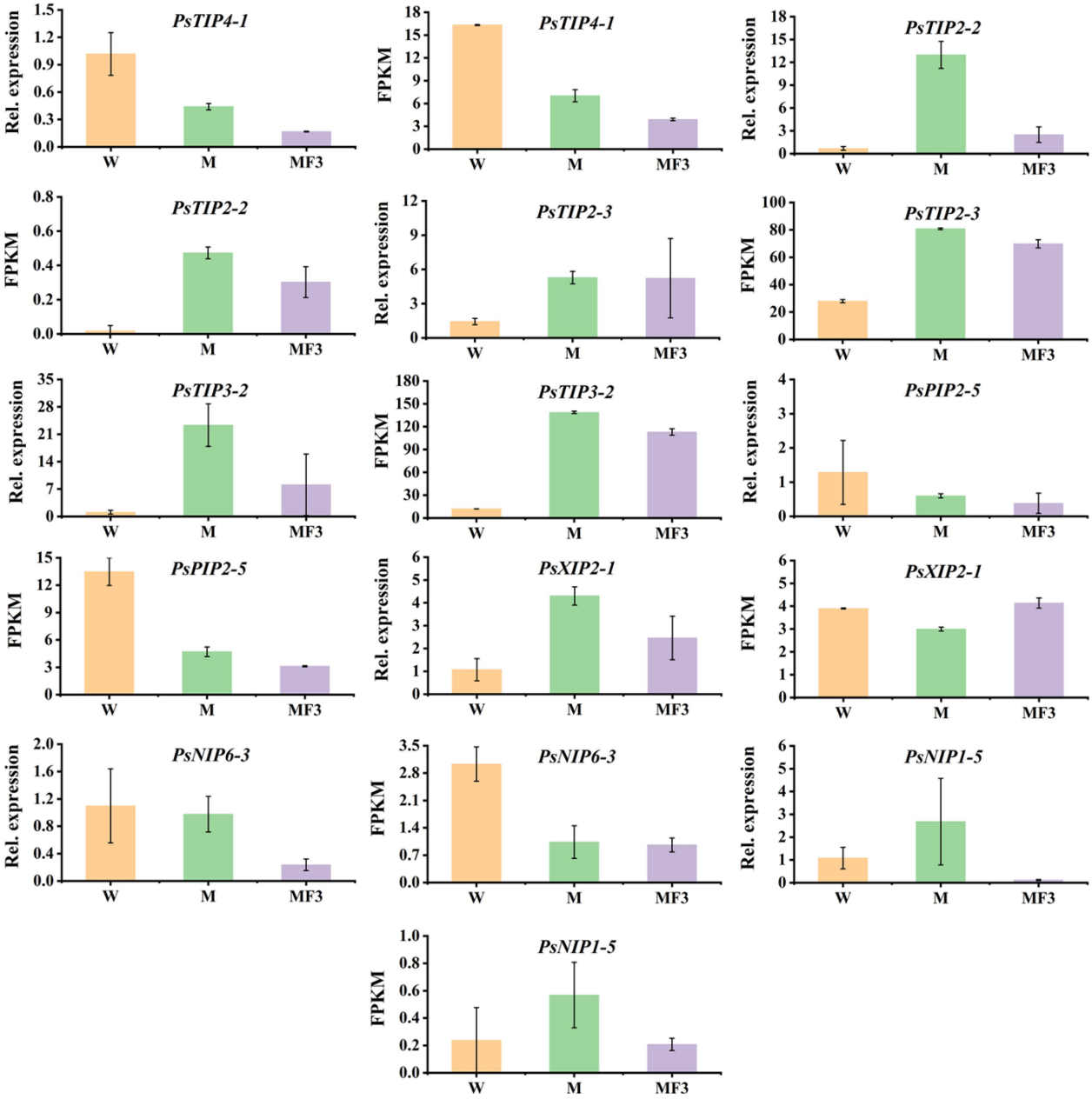


**Fig. 7** The expression patterns of seven *PsAQPs* in imbibing seeds as revealed by RNA-Seq and qRT-PCR. The seeds were sampled after 12 h soaking in three different solutions, namely water (W), 0.3 M mannitol (M), and 100 mg/L fullerol dissolved in 0.3 M mannitol (MF3) solution. Error bars are standard errors calculated from three replicates.

## Conflict of interest

Pei Xu is the Editorial Board member of journal *Vegetable Research*. He was blinded from reviewing or making decisions on the manuscript. The article was subject to the journal's standard procedures, with peer-review handled independently of this Editorial Board member and his research group.

**Supplementary Information** accompanies this paper at (https://www.maxapress.com/article/doi/10.48130/VR-2023-0010)

## Dates

Received 22 November 2022; Accepted 16 January 2023; Published online 14 March 2023

## REFERENCES

1. Fox AR, Maistriaux LC, Chaumont F. 2017. Toward understanding of the high number of plant aquaporin isoforms and multiple regulation mechanisms. *Plant Science* 264:179–87
2. Chaumont F, Tyerman SD. 2014. Aquaporins: highly regulated channels controlling plant water relations. *Plant Physiology* 164:1600–18
3. Johanson U, Karlsson M, Johansson I, Gustavsson S, Sjövall S, et al. 2001. The complete set of genes encoding major intrinsic proteins in Arabidopsis provides a framework for a new nomenclature for major intrinsic proteins in plants. *Plant Physiology* 126:1358–69
4. Sakurai J, Ishikawa F, Yamaguchi T, Uemura M, Maeshima M. 2005. Identification of 33 rice aquaporin genes and analysis of their expression and function. *Plant and Cell Physiology* 46:1568–77

5. Zhang D, Ali Z, Wang C, Xu L, Yi J, et al. 2013. Genome-wide sequence characterization and expression analysis of major intrinsic proteins in soybean (*Glycine max* L.). *PLoS One* 8:e56312
6. Deshmukh RK, Vivancos J, Guérin V, Sonah H, Labbé C, et al. 2013. Identification and functional characterization of silicon transporters in soybean using comparative genomics of major intrinsic proteins in Arabidopsis and rice. *Plant Molecular Biology* 83:303–15
7. Deokar AA, Tar'An B. 2016. Genome-wide analysis of the aquaporin gene family in chickpea (*Cicer arietinum* L.). *Frontiers in Plant Science* 7:1802
8. Shivaraj SM, Deshmukh R, Sonah H, Bélanger RR. 2019. Identification and characterization of aquaporin genes in *Arachis duranensis* and *Arachis ipaensis* genomes, the diploid progenitors of peanut. *BMC Genomics* 20:222
9. De Rosa A, Watson-Lazowski A, Evans JR, Groszmann M. 2020. Genome-wide identification and characterisation of Aquaporins in *Nicotiana tabacum* and their relationships with other Solanaceae species. *BMC Plant Biology* 20:266
10. Kruse E, Uehlein N, Kaldenhoff R. 2006. The aquaporins. *Genome Biology* 7:206
11. Ishikawa F, Suga S, Uemura T, Sato MH, Maeshima M. 2005. Novel type aquaporin SIPs are mainly localized to the ER membrane and show cell-specific expression in Arabidopsis thaliana. *FEBS Letters* 579:5814–20
12. Fortin MG, Morrison NA, Verma DP. 1987. Nodulin-26, a peribacteroid membrane nodulin is expressed independently of the development of the peribacteroid compartment. *Nucleic Acids Research* 15:813–24
13. Kapilan R, Vaziri M, Zwiazek JJ. 2018. Regulation of aquaporins in plants under stress. *Biological Research* 51:4
14. Clarkson DT, Carvajal M, Henzler T, Waterhouse RN, Smyth AJ, et al. 2000. Root hydraulic conductance: diurnal aquaporin expression and the effects of nutrient stress. *Journal of Experimental Botany* 51:61–70
15. Maurel C, Boursiac Y, Luu DT, Santoni V, Shahzad Z, et al. 2015. Aquaporins in plants. *Physiological Reviews* 95:1321–58
16. Cui X, Hao F, Chen H, Chen J, Wang X. 2008. Expression of the Vicia faba *VfPIP1* gene in *Arabidopsis thaliana* plants improves their drought resistance. *Journal of Plant Research* 121:207–14
17. Ranganathan K, El Kayal W, Cooke JEK, Zwiazek JJ. 2016. Responses of hybrid aspen over-expressing a PIP2;5 aquaporin to low root temperature. *Journal of Plant Physiology* 192:98–104
18. Sakurai-Ishikawa JU, Murai-Hatano MA, Hayashi H, Ahamed A, Fukushi K, et al. 2011. Transpiration from shoots triggers diurnal changes in root aquaporin expression. *Plant, Cell & Environment* 34:1150–63
19. Nada RM, Abogadallah GM. 2014. Aquaporins are major determinants of water use efficiency of rice plants in the field. *Plant Science* 227:165–80
20. Wang L, Zhang C, Wang Y, Wang Y, Yang C, et al. 2018. *Tamarix hispida* aquaporin *ThPIP2;5* confers salt and osmotic stress tolerance to transgenic *Tamarix* and *Arabidopsis*. *Environmental and Experimental Botany* 152:158–66
21. Wang L, Li Q, Lei Q, Feng C, Zheng X, et al. 2017. Ectopically expressing MdPIP1; 3, an aquaporin gene, increased fruit size and enhanced drought tolerance of transgenic tomatoes. *BMC Plant Biology* 17:246
22. Wang X, Li Y, Ji W, Bai X, Cai H, et al. 2011. A novel *Glycine soja* tonoplast intrinsic protein gene responds to abiotic stress and depresses salt and dehydration tolerance in transgenic *Arabidopsis thaliana*. *Journal of Plant Physiology* 168:1241–48
23. Maiti D, Tong X, Mou X, Yang K. 2019. Carbon-based nanomaterials for biomedical applications: a recent study. *Frontiers in Pharmacology* 9:1401
24. Khodakovskaya M, Dervishi E, Mahmood M, Xu Y, Li Z, et al. 2009. Carbon nanotubes are able to penetrate plant seed coat and dramatically affect seed germination and plant growth. *ACS Nano* 3:3221–27
25. Burman U, Kumar P. 2018. Plant response to engineered nanoparticles. In *Nanomaterials in Plants, Algae, and Microorganisms*, eds. Tripathi DK, Ahmad P, Sharma S, Chauhan DK, Dubey NK. London, United Kingdom: Academic Press. pp. 103–18. https://doi.org/10.1016/B978-0-12-811487-2.00005-0
26. Ali S, Mehmood A, Khan N. 2021. Uptake, translocation, and consequences of nanomaterials on plant growth and stress adaptation. *Journal of Nanomaterials* 2021:6677616
27. Qin Y. 2016. Medical textile materials with drug-releasing properties. In *Medical Textile Materials*. pp. 175–89.
28. Xiao L, Takada H, Gan X, Miwa N. 2006. The water-soluble fullerene derivative 'Radical Sponge®'exerts cytoprotective action against UVA irradiation but not visible-light-catalyzed cytotoxicity in human skin keratinocytes. *Bioorganic & Medicinal Chemistry Letters* 16:1590–95
29. Krokosz A. 2007. Fullerenes in biology. *Postepy Biochemii* 53:91–96
30. Kole C, Kole P, Randunu KM, Choudhary P, Podila R, et al. 2013. Nanobiotechnology can boost crop production and quality: first evidence from increased plant biomass, fruit yield and phytomedicine content in bitter melon (*Momordica charantia*). *BMC Biotechnology* 13:37
31. Husen A, Siddiqi KS. 2014. Carbon and fullerene nanomaterials in plant system. *Journal of Nanobiotechnology* 12:16
32. Panova GG, Ktitorova IN, Skobeleva OV, Sinjavina NG, Charykov NA, et al. 2016. Impact of polyhydroxy fullerene (fullerol or fullerenol) on growth and biophysical characteristics of barley seedlings in favourable and stressful conditions. *Plant Growth Regulation* 79:309–17
33. Arruda SCC, Silva ALD, Galazzi RM, Azevedo RA, Arruda MAZ. 2015. Nanoparticles applied to plant science: a review. *Talanta* 131:693–705
34. Samadi S, Asgari Lajayer B, Moghiseh E, Rodríguez-Couto S. 2021. Effect of carbon nanomaterials on cell toxicity, biomass production, nutritional and active compound accumulation in plants. *Environmental Technology & Innovation* 21:101323
35. Kreplak J, Madoui MA, Cápal P, Novák P, Labadie K, et al. 2019. A reference genome for pea provides insight into legume genome evolution. *Nature Genetics* 51:1411–22
36. Tamura K, Stecher G, Peterson D, Filipski A, Kumar S. 2013. MEGA6: molecular evolutionary genetics analysis version 6.0. *Molecular Biology and Evolution* 30:2725–29
37. Marchler-Bauer A, Derbyshire MK, Gonzales NR, Lu S, Chitsaz F, Geer LY, Geer RC, He J, Gwadz M, Hurwitz DI, Lanczycki CJ. 2015. CDD: NCBI's conserved domain database. *Nucleic Acids Research* 43:D222–D226
38. Krogh A, Larsson B, Von Heijne G, Sonnhammer EL. 2001. Predicting transmembrane protein topology with a hidden Markov model: application to complete genomes. *Journal of Molecular Biology* 305:567–80
39. Stothard P. 2000. The sequence manipulation suite: JavaScript programs for analyzing and formatting protein and DNA sequences. *BioTechniques* 28:1102–4
40. Chou KC, Shen HB. 2010. Plant-mPLoc: A top-down strategy to augment the power for predicting plant protein subcellular localization. *PLoS One* 5:e11335
41. Horton P, Park KJ, Obayashi T, Fujita N, Harada H, et al. 2007. WoLF PSORT: protein localization predictor. *Nucleic Acids Research* 35:W585–W587
42. Hu B, Jin J, Guo A, Zhang H, Luo J, et al. 2015. GSDS 2.0: an upgraded gene feature visualization server. *Bioinformatics* 31:1296–97
43. Kim D, Pertea G, Trapnell C, Pimentel H, Kelley R, et al. 2013. TopHat2: accurate alignment of transcriptomes in the presence of insertions, deletions and gene fusions. *Genome Biology* 14:R36
44. Trapnell C, Roberts A, Goff L, Pertea G, Kim D, et al. 2012. Differential gene and transcript expression analysis of RNA-seq experiments with TopHat and Cufflinks. *Nature Protocols* 7:562–78

45. Savage DF, O'Connell JD III, Miercke LJW, Finer-Moore J, Stroud RM. 2010. Structural context shapes the aquaporin selectivity filter. *Proceedings of the National Academy of Sciences* 107:17164–69
46. Sui H, Han BG, Lee JK, Walian P, Jap BK. 2001. Structural basis of water-specific transport through the AQP1 water channel. *Nature* 414:872–78
47. Deshmukh RK, Vivancos J, Ramakrishnan G, Guérin V, Carpentier G, et al. 2015. A precise spacing between the NPA domains of aquaporins is essential for silicon permeability in plants. *The Plant Journal* 83:489–500
48. Ariani A, Gepts P. 2015. Genome-wide identification and characterization of aquaporin gene family in common bean (*Phaseolus vulgaris* L.). *Molecular Genetics and Genomics* 290:1771–85
49. Min X, Wu H, Zhang Z, Wei X, Jin X, et al. 2019. Genome-wide identification and characterization of the aquaporin gene family in *Medicago truncatula*. *Journal of Plant Biochemistry and Biotechnology* 28:320–35
50. Reuscher S, Akiyama M, Mori C, Aoki K, Shibata D, et al. 2013. Genome-wide identification and expression analysis of aquaporins in tomato. *PLoS One* 8:e79052
51. Lee JK, Kozono D, Remis J, Kitagawa Y, Agre P, et al. 2005. Structural basis for conductance by the archaeal aquaporin AqpM at 1.68 Å. *PNAS* 102:18932–37
52. Porcel R, Bustamante A, Ros R, Serrano R, Mulet Salort JM. 2018. BvCOLD1: a novel aquaporin from sugar beet (*Beta vulgaris* L.) involved in boron homeostasis and abiotic stress. *Plant, Cell & Environment* 41:2844–57
53. Coskun D, Deshmukh R, Sonah H, Menzies JG, Reynolds O, et al. 2019. The controversies of silicon's role in plant biology. *New Phytologist* 221:67–85
54. Zhang N, Deyholos MK. 2016. RNASeq analysis of the shoot apex of flax (*Linum usitatissimum*) to identify phloem fiber specification genes. *Frontiers in Plant Science* 7:950
55. Sonah H, Deshmukh RK, Labbé C, Bélanger RR. 2017. Analysis of aquaporins in Brassicaceae species reveals high-level of conservation and dynamic role against biotic and abiotic stress in canola. *Scientific Reports* 7:2771
56. Xiong J, Li J, Wang H, Zhang C, Naeem MS. 2018. Fullerol improves seed germination, biomass accumulation, photosynthesis and antioxidant system in *Brassica napus* L. under water stress. *Plant Physiology and Biochemistry* 129:130–40
57. Toscano S, Romano D, Tribulato A, Patanè C. 2017. Effects of drought stress on seed germination of ornamental sunflowers. *Acta Physiologiae Plantarum* 39:184
58. Suga S, Komatsu S, Maeshima M. 2002. Aquaporin isoforms responsive to salt and water stresses and phytohormones in radish seedlings. *Plant and Cell Physiology* 43:1229–37
59. Rodrigues MI, Bravo JP, Sassaki FT, Severino FE, Maia IG. 2013. The tonoplast intrinsic aquaporin (TIP) subfamily of *Eucalyptus grandis*: characterization of *EgTIP2*, a root-specific and osmotic stress-responsive gene. *Plant Science* 213:106–13
60. Béré E, Lahbib K, Merceron B, Fleurat-Lessard P, Boughanmi NG. 2017. $\alpha$-TIP aquaporin distribution and size tonoplast variation in storage cells of *Vicia faba* cotyledons at seed maturation and germination stages. *Journal of Plant Physiology* 216:145–51